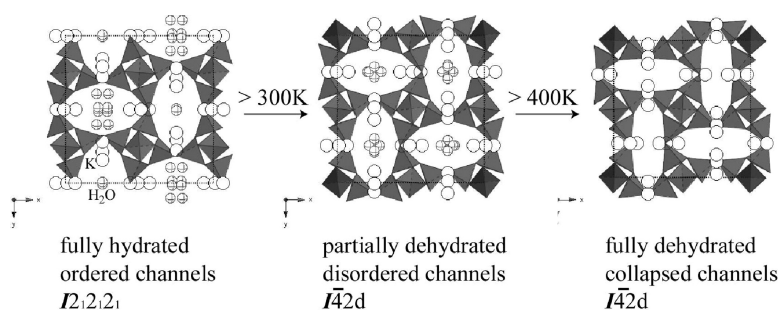


## Dehydration-Induced Water Disordering in a Synthetic Potassium Gallosilicate Natrolite

Yongjae Lee, Sun Jin Kim, Ivor Bull, Aaron J. Celestian, John B. Parise, Chi-Chang Kao, and Thomas Vogt

*J. Am. Chem. Soc.*, **2007**, 129 (44), 13744-13748 • DOI: 10.1021/ja075037z • Publication Date (Web): 13 October 2007

Downloaded from <http://pubs.acs.org> on February 14, 2009



### More About This Article

Additional resources and features associated with this article are available within the HTML version:

- Supporting Information
- Links to the 2 articles that cite this article, as of the time of this article download
- Access to high resolution figures
- Links to articles and content related to this article
- Copyright permission to reproduce figures and/or text from this article

[View the Full Text HTML](#)



## Dehydration-Induced Water Disordering in a Synthetic Potassium Gallosilicate Natrolite

Yongjae Lee,<sup>\*,†</sup> Sun Jin Kim,<sup>‡</sup> Ivor Bull,<sup>§</sup> Aaron J. Celestian,<sup>||</sup> John B. Parise,<sup>⊥</sup> Chi-Chang Kao,<sup>○</sup> and Thomas Vogt<sup>#</sup>

Contribution from the Department of Earth System Sciences, Yonsei University, Seoul 120-749, Korea, Nano-Materials Research Center, Korea Institute of Science and Technology, Seoul 136-791, Korea, BASF CATALYSTS LLC, 101 Wood Avenue, P.O. Box 770, Iselin, New Jersey 08830, Department of Geography and Geology, Western Kentucky University, Bowling Green, Kentucky 42101, Department of Geosciences, State University of New York, Stony Brook, New York 11794, National Synchrotron Light Source, Brookhaven National Laboratory, Upton, New York 11973, and NanoCenter and Department of Chemistry and Biochemistry, University of South Carolina, Columbia, South Carolina 29208

Received July 8, 2007; E-mail: yongjaelee@yonsei.ac.kr

**Abstract:** A new potassium gallosilicate zeolite with a natrolite topology (approximate formula  $K_{8.2}Ga_{8.2}Si_{11.8}O_{40} \cdot 11.5H_2O$ ) was synthesized under hydrothermal conditions and characterized as a function of temperature using monochromatic synchrotron X-ray powder diffraction and Rietveld analyses. Unlike the previously known tetragonal  $K_8Ga_8Si_{12}O_{40} \cdot 6H_2O$  phase, the as-synthesized material contains twice the amount of water molecules in an ordered arrangement throughout the channels in an orthorhombic ( $I2_12_12_1$ ) symmetry. The ordered configuration of water molecules is stabilized below 300 K, whereas heating above 300 K results in a selective dehydration and subsequent disordering of water molecules in a tetragonal ( $I42d$ ) symmetry. Above 400 K, the material transforms to a fully dehydrated tetragonal phase with a concomitant volume reduction of ca. 15%. The fully dehydrated material transforms back to its original state when rehydrated over a period of up to 2 weeks. The distribution of potassium cations within the channels remains largely unperturbed during the water rearrangements and their order–disorder transition within the channels.

### Introduction

Zeolites crystallize in a variety of low-density framework structures composed of corner-connected networks of  $(Al, SiO_4)$ -tetrahedra, which enclose well-defined pores of molecular dimensions containing charge-balancing cations and molecules such as water.<sup>1</sup> The restricted access to the interior, providing reactant, transition state, and product selectivity, makes these “nanoreactors” valuable selective heterogeneous catalysts and ion exchangers used in a number of industrial and environmental applications. The built-in flexibility of the T–O–T angle connecting the tetrahedral units allows these structures to contract and expand in response to thermodynamic variables such as temperature and pressure. Numerous variable-temperature studies show that cations can migrate within the pores and water content varies usually with a concomitant relaxation of the framework.<sup>2–5</sup> In recent studies, we have identified the

unique role of pressure in controlling the zeolitic water content. In sodium aluminosilicate natrolite, the application of hydrostatic pressure using an ethanol–methanol–water mixture (used as a pressure transmitting fluid) leads to anomalous swelling of the unit cell volume and increase in the crystal water content (pressure-induced hydration, PIH).<sup>6,7</sup> We have investigated other related synthetic variants, and interestingly, a different behavior of the PIH was found in each compositionally altered material, including irreversible PIH<sup>8</sup> and the reduction of the onset pressure of PIH.<sup>9</sup> In all cases, the initial water content and its dispersal were found to be crucial to the pressure-induced hydration of the natrolite framework.

In an attempt to further understand the interplay between water and the natrolite framework and to provide a structural base from which to interpret pressure-induced hydration, we

<sup>†</sup> Yonsei University.

<sup>‡</sup> Korea Institute of Science and Technology.

<sup>§</sup> BASF CATALYSTS LLC.

<sup>||</sup> Western Kentucky University.

<sup>⊥</sup> State University of New York.

<sup>○</sup> Brookhaven National Laboratory.

<sup>#</sup> University of South Carolina.

(1) Breck, D. W. *Zeolite Molecular Sieves*; Krieger: Malabar, FL, 1984.

(2) Artioli, G.; Stahl, K.; Hanson, J. C. *Mater. Sci. Forum* **1996**, 228–231, 369.

(3) Baur, W. H.; Joswig, W. N. *Jb. Miner. Mh.* **1996**, 171–187.

(4) Nair, S.; Tsapatsis, M.; Toby, B. H.; Kuznicki, S. M. *J. Am. Chem. Soc.* **2001**, 123, 12781–12790.

(5) Lee, Y.; Reisner, B. A.; Hanson, J. C.; Jones, G. A.; Parise, J. B.; Corbin, D. R.; Toby, B. H.; Freitag, A.; Larese, J. Z.; Kahlenberg, V. *J. Phys. Chem.* **2001**, B105, 7188–7199.

(6) Lee, Y.; Hriljac, J. A.; Vogt, T.; Parise, J. B.; Artioli, G. *J. Am. Chem. Soc.* **2001**, 123, 12732–12733.

(7) Lee, Y.; Vogt, T.; Hriljac, J. A.; Parise, J. B.; Artioli, G. *J. Am. Chem. Soc.* **2002**, 124, 5466–5475.

(8) Lee, Y.; Vogt, T.; Hriljac, J. A.; Parise, J. B.; Hanson, J. C.; Kim, S. J. *Nature* **2002**, 420, 485–489.

(9) Lee, Y.; Hriljac, J. A.; Kim, S.-J.; Hanson, J. C.; Vogt, T. *J. Am. Chem. Soc.* **2003**, 125, 6036–6037.

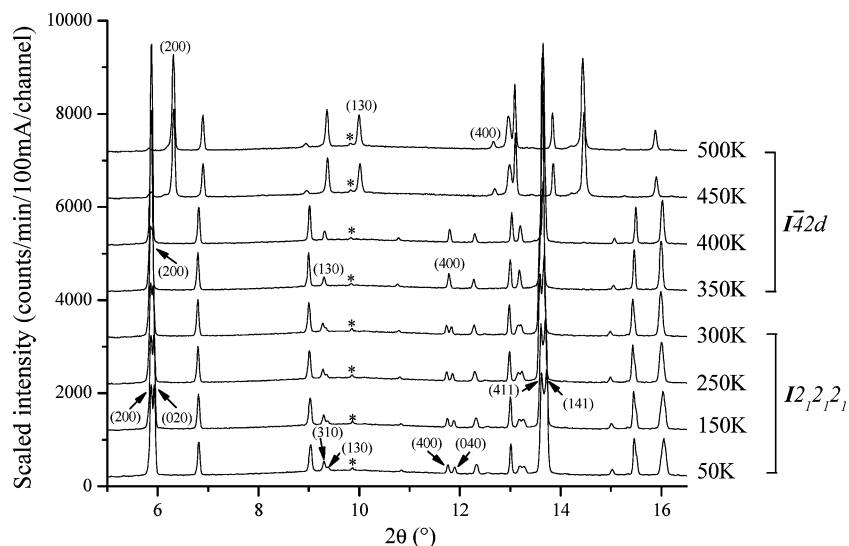


**Figure 1.** Changes in the synchrotron X-ray powder diffraction patterns observed for  $\text{K}_{8.2}\text{Ga}_{8.2}\text{Si}_{11.8}\text{O}_{40}\cdot 11.5\text{H}_2\text{O}$  as a function of temperature. \* = Impurity peak.

have undertaken the systematic synthesis of different gallosilicate natrolites and characterized their structures as a function of temperature using monochromatic synchrotron X-ray powder diffraction and Rietveld analyses. We find that by introducing a small variation in the synthesis gel composition, a new potassium gallosilicate natrolite can crystallize in an orthorhombic ( $I2_12_12_1$ ) unit cell with the water content similar to that found in tetragonal K-GaSi-NAT in its “superhydrated” PIH state (12  $\text{H}_2\text{O}$  per 40 framework O atoms,  $\text{O}_f$ ).<sup>8</sup> This newly synthesized phase, with a water content greater than the normal 6 $\text{H}_2\text{O}$  per 40  $\text{O}_f$ ,<sup>10</sup> distinguishes itself by having water molecules distributed in an ordered arrangement over the available sites along the channels. Such a “water-ordered” configuration converts to a “water-disordered” one by a postsynthesis tempering which induces water diffusion across the channels. The evolution of the water network as a function of temperature in this new synthetic potassium gallosilicate is discussed here in relation to the resulting water order–disorder transition and the framework collapse via dehydration.

## Experimental Section

**Synthesis.** K-GaSi-NAT-ort was synthesized using a hydrothermal method from a gel with the composition of 3.5  $\text{K}_2\text{O}$ :1.0  $\text{Ga}_2\text{O}_3$ :3.0  $\text{SiO}_2$ :80  $\text{H}_2\text{O}$ . A mixture of 0.94 g of  $\text{Ga}_2\text{O}_3$  (Aldrich), 4.36 g of KOH (45 wt % in  $\text{H}_2\text{O}$ , Fisher), and 3.45 mL of deionized water was heated at 110 °C for approximately 16 h in a polypropylene bottle. After cooling to room temperature, 2.25 g of colloidal silica (Ludox AS 40, Aldrich) were added dropwise to the solution while stirring for 4 h. The resulting clear solution was heated in a Teflon-lined vessel at 110 °C for 5 days. The products was recovered by filtration, washed with deionized water, and dried at room temperature. Initial characterization of the bulk sample to verify phase identity, establish phase purity, and determine preliminary indexing was done by powder X-ray diffraction using a Scintag PAD-X automated diffractometer. The Ga/Si ratio of ca. 2/3 was confirmed using a LEO 1550 scanning electron microscope using a Phoenix/Sapphire EDAX attachment. TGA, performed on an equilibrated sample under dry-Ar flow, showed an overall ~7.3 wt % loss in the temperature range between RT and 150 °C (see figures in Supporting Information).

**Synchrotron X-ray Powder Diffraction.** High-resolution synchrotron X-ray powder diffraction data of K-GaSi-NAT-ort were measured at beamline X7A at the National Synchrotron Light Source (NSLS) at Brookhaven National Laboratory. The powdered sample was loaded into a glass capillary of 0.3 mm diameter, which was then sealed and mounted on the second axis of the diffractometer. A monochromatic beam was obtained using a channel-cut Ge(111) single crystal, and a wavelength of 0.7051(1) Å was calibrated using a  $\text{CeO}_2$  standard (SRM 674). A gas-proportional position-sensitive detector (PSD), gated at the Kr-escape peak, was employed for high-resolution ( $\Delta d/d \approx 10^{-3}$ ) powder diffraction data measurements.<sup>11</sup> The PSD was stepped in 0.25° intervals between 5° and 43° in  $2\theta$  with increasing counting time at higher angles, and the capillary was spun during the measurement for better powder averaging.

Variable temperature X-ray powder diffraction measurements were also performed at beamline X7A at the NSLS. The powdered sample was loaded into a glass capillary of 0.3 mm diameter. The capillary was cut to expose the sample to the surrounding environment for the ease of *in situ* dehydration. A monochromatic beam of 0.7040(1) Å was selected using a channel-cut Ge(111) single crystal. The capillary sample was mounted on the second axis of the diffractometer inside a modified closed-cycle He cryostat, which has an absolute temperature accuracy of  $\pm 5$  K and a stability better than 0.1 K. Diffraction data were measured at 50 K using a PSD stepped in 0.25° intervals over the angular range 5°–35° in  $2\theta$  with counting times of 60 s per step. The sample temperature was then increased by 50 K intervals up to 550 K for subsequent data measurements. The cryostat was rocked by 5° during data collection in order to obtain a better powder averaging. The resulting X-ray powder diffraction patterns are shown in Figure 1.

When measured using an in-house X-ray diffractometer, the powder diffraction pattern of the as-synthesized K-GaSi-NAT-ort is very similar to the original  $\text{K}_8\text{Ga}_8\text{Si}_{12}\text{O}_{40}\cdot 6\text{H}_2\text{O}$  phase and can be indexed with a tetragonal unit cell in space group  $I42d$  ( $a \approx 13.74$  Å,  $c \approx 6.59$  Å). High-resolution synchrotron X-ray diffraction data taken at room temperature, however, reveal a subtle splitting of the (040) peak in the K-GaSi-NAT-ort sample (Figure 1); it also indicated the presence of impurity peaks, most noticeably near 10° in  $2\theta$  with ca. 2% intensity of the strongest reflection from the main phase. Subsequently, an orthorhombic cell was successfully used to index the diffraction pattern. The space group  $I2_12_12_1$ , a subgroup of  $I42d$ , was used to construct the starting framework model. In the variable temperature measure-

(10) Lee, Y.; Kim, S. J.; Parise, J. B. *Microporous Mesoporous Mater.* **2000**, *34*, 255–271.

(11) Smith, G. C. *Synch. Rad. News* **1991**, *4*, 24–30.

ments, a small degree of anisotropic peak broadening was noticed to develop in the high-temperature region where a tetragonal cell is observed upon dehydration. Rietveld structure refinements were performed using the GSAS suite of programs.<sup>12,13</sup> Difference Fourier maps were generated, and potassium and oxygen atoms were used to account for the nonframework species  $K^+$  and water molecules, respectively. Fractional site occupancies of nonframework oxygen were refined to model the water content at different temperatures. The sum of site occupancies for the K1 and K2 sites was constrained to be unity from the 50 K to 300 K models. An overall isotropic displacement parameter was used for the framework atoms; another set was used to constrain the nonframework oxygen and potassium. Framework models above 450 K were derived from DLS minimization<sup>14,15</sup> and fixed during the refinement. Selected refinement results for both the as-synthesized and in situ variable temperature structure models are listed in Supplementary Tables 1 and 2 (Supporting Information), and the temperature evolutions of the unit cell volume and edge lengths are shown in Figure 2.

## Results and Discussion

**Room-Temperature Structure Model of the As-Synthesized K-GaSi-NAT-ort.** Subtle variations in the synthesis conditions can have a large influence on the resulting natrolite framework. For instance, Cho et al. first prepared two different sodium gallosilicate natrolites (TNU-3 and TNU-4) from the same gel composition and reaction times and attributed the resulting difference in the framework ordering to using different crystallization temperatures.<sup>16</sup> Recently, Hong et al. found that the framework ordering is energetically favored when  $Si/Ga \approx 1.5$  and the degree of ordering can be tailored by quenching the crystallization gel at different reaction times.<sup>17</sup> In sodium gallosilicates, the degree of framework ordering was also found to influence the zeolitic water content at ambient conditions. During our efforts to synthesize potassium forms of gallosilicate natrolite, a new structure with a higher water content than the one previously known in the tetragonal  $K_8Ga_8Si_{12}O_{40} \cdot 6H_2O$  phase was found as a result of small variations in the gel composition used for the synthesis. The structural model of K-GaSi-NAT-ort, depicted in Figure 3, shows the arrangement of water molecules hitherto unknown inside the natrolite channels along the  $c$ -axis. Compared to the water arrangements found in either the original tetragonal K-GaSi-NAT<sup>10</sup> or its high-pressure variant,<sup>8</sup> the orthorhombic variant of K-GaSi-NAT-ort exhibits a different distribution of the water molecules throughout the channels; one set of channels contains disordered OW2 and OW3 water molecules while the neighboring ones contain only OW1 water molecules near the center of the channel. We refer to this water network as “water-ordered” compared to the “water-disordered” one found in the tetragonal K-GaSi-NAT phases. The amount of water molecules derived from the refinement is 11.5(5) per unit cell, which amounts to ca. 10 wt %. The weight loss measured from TGA is, however, only 7.3 wt %. The difference may be partly due to the presence

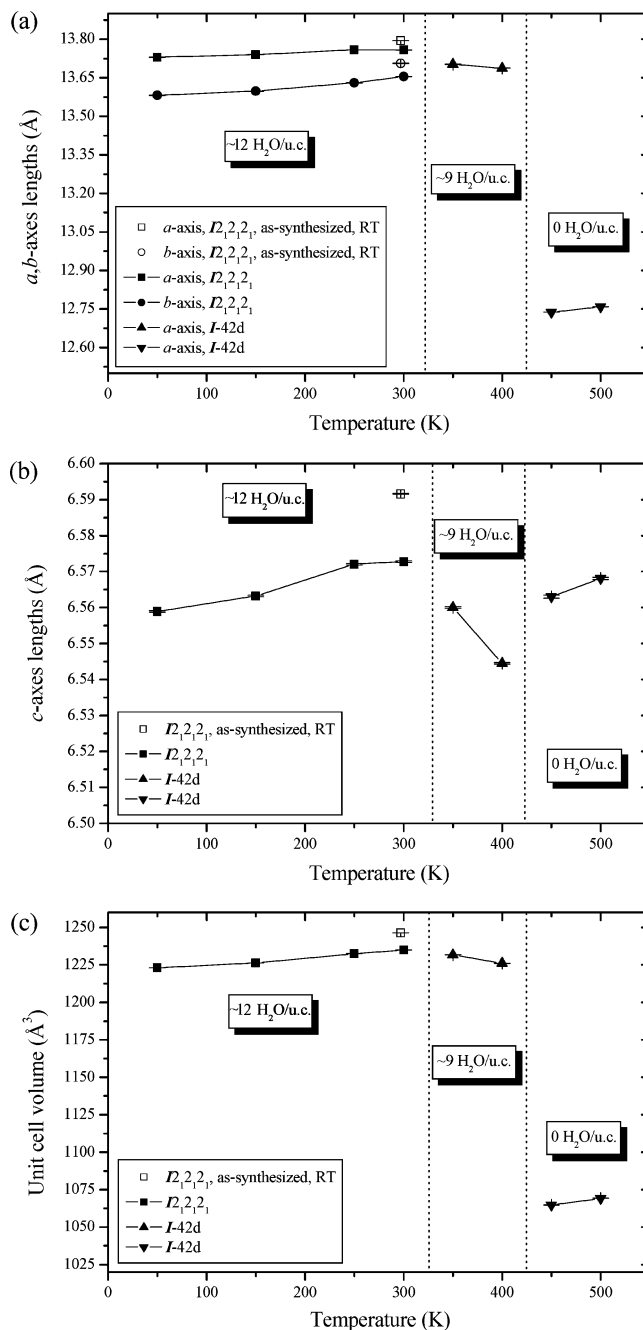


**Figure 2.** Temperature dependence of the (a and b) unit cell edge lengths and (c) volume for  $K_{8.2}Ga_{8.2}Si_{11.8}O_{40} \cdot 11.5H_2O$ . The water content per unit cell (per 40 framework oxygen atoms) is also shown in the insets.

of an impurity phase, but we suspect the main reason to be partial dehydration of the sample while it is stored under a dry-Ar environment prior to the TG scan. As described in the next section, structural changes occur near room temperature; heating below 400 K results in partial dehydration and subsequent water disordering in the channels whereas the water ordering is stabilized via cooling.

**Variable-Temperature Structure Models.** At temperatures below 300 K, K-GaSi-NAT-ort maintains an ordered arrangement of water molecules over the different sites in the channels; the splitting between the (040) and (400) reflections increases further as the temperature decreases (Figures 1 and 2). The unit cell volume as well as the individual unit cell lengths exhibit a normal thermal expansion as expected with no apparent

(12) Larson, A. C.; VonDreele, R. B. “GSAS; General Structure Analysis System,” Report LAUR 86-748, Los Alamos National Laboratory, New Mexico, 1986.

(13) Toby, B. H. *J. Appl. Crystallogr.* **2001**, *34*, 210–213.

(14) Baur, W. H. *Phys. Chem. Miner.* **1977**, *2*, 3.

(15) Lee, Y.; Vogt, T.; Hriljac, J. A.; Parise, J. B. *Chem. Mater.* **2002**, *14*, 3501–3508.

(16) Cho, H. H.; Kim, S. H.; Kim, Y. G.; Kim, Y. C.; Koller, H.; Cambor, M. A.; Hong, S. B. *Chem. Mater.* **2000**, *12*, 2292–2300.

(17) Hong, S. B.; Lee, S.-H.; Shin, C.-H.; Woo, A. J.; Alvarez, L. J.; Zicovich-Wilson, C. M.; Cambor, M. A. *J. Am. Chem. Soc.* **2004**, *126*, 13742–13751.



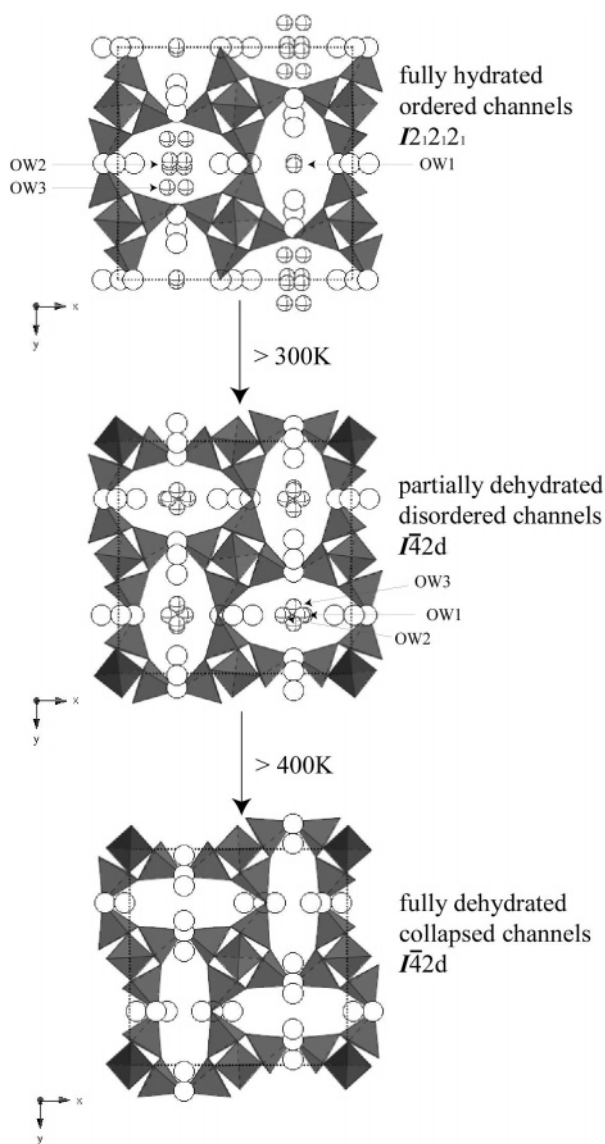


**Figure 3.** Temperature evolution of the structural models of  $K_{8.2}Ga_{8.2}Si_{11.8}O_{40} \cdot 11.5H_2O$ . Large-empty and small-stripped circles represent potassium cations and water molecules, respectively. Ga/Si atoms are disordered over sites centered on the dark corner-connected tetrahedra constituting the framework. Dotted lines outline the unit cell.

compositional changes during heating from 20 K (Figure 2). The unit cell volume, measured after heating back to 300 K, is slightly smaller, i.e., by 0.9%, than the one measured before the temperature cycle.

As the temperature increases above 300 K, K-GaSi-NAT-ort loses water (by ca.  $\sim 2 H_2O$  per 40  $O_f$  at 400 K) and transforms to a tetragonal structure with a disordered water assembly throughout the channels (Figures 3 and 4). This partial dehydration causes only a minor unit cell volume contraction ( $\sim 0.7\%$ ). A further increase of the temperature above 400 K results in complete dehydration, and the unit cell volume contracts by as much as 15% (Figures 2 and 3). The anhydrous tetragonal phase exhibits the most elliptical channel openings along the  $c$ -axis with a longer-to-shorter oxygen–oxygen diagonal distance ratio of 2.23, compared to 1.55 observed at 300 K for K-GaSi-NAT-ort (Figure 3). The potassium cation distributions show only minor rearrangements throughout the entire temperature range and during the water order–disorder

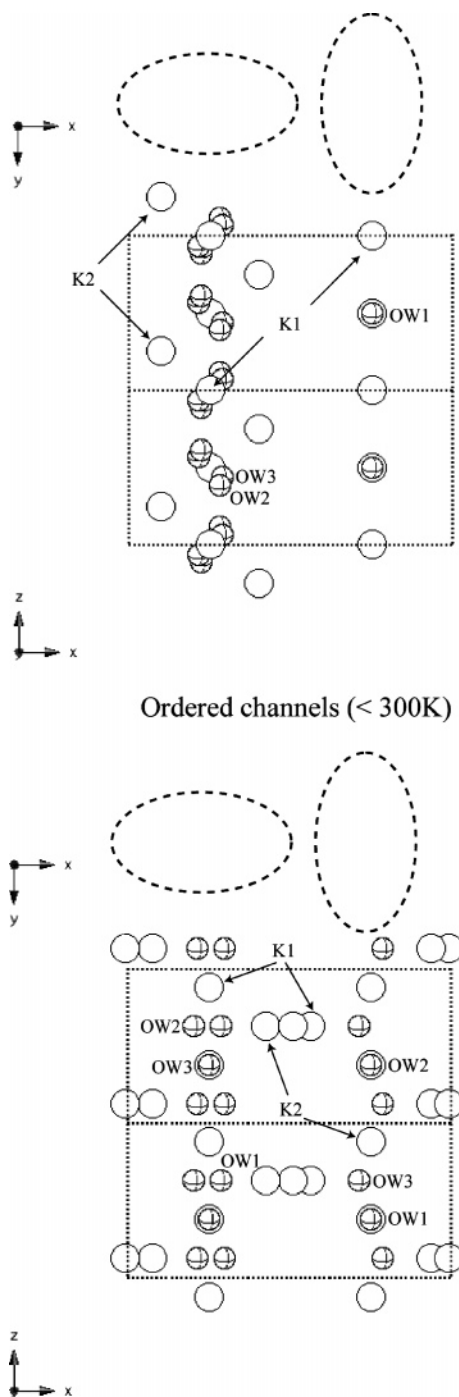


**Figure 4.** Schematic comparisons between water-ordered and disordered channels viewed along the  $b$ -axis. Large-empty and small-stripped circles represent potassium cations and water molecules, respectively. Framework tetrahedra and some of the intrachannel species are omitted for clarity. Dotted lines outline the unit cell. Relative orientations of the elliptical channels outlined by the corner-connected tetrahedra are shown above.

transition (Figures 3 and 4). When the fully dehydrated sample is cooled down and exposed to air, rehydration takes place, and the material transforms back to its original state within a week or two when exposed to the humidity conditions of the laboratory ( $\sim 20\%$  R.H.).

The water order–disorder transition observed at temperatures above 300 K involves the selective dehydration and interchannel

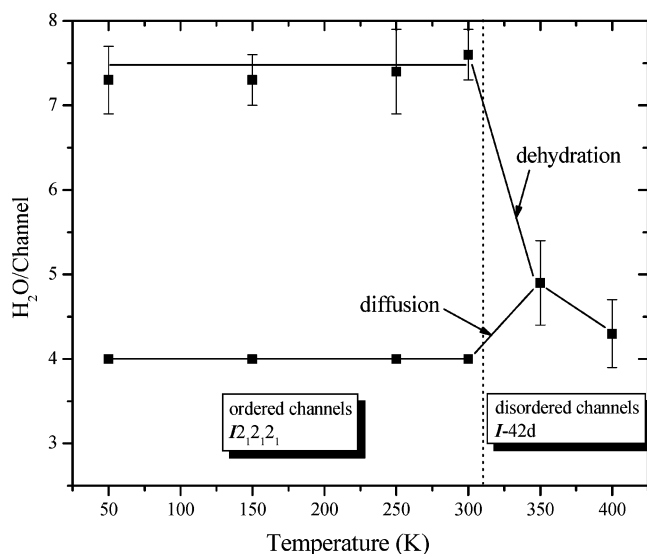


**Figure 5.** Temperature dependence of the water contents in the channels of  $K_{8.2}Ga_{8.2}Si_{11.8}O_{40} \cdot 11.5H_2O$ . Two different water contents per channel below 300 K represent the ordered state, which transforms to the disordered state above 300 K to show uniform distribution of water molecules.

diffusion of water molecules; below 300 K, the water molecules preferentially occupy one set of channels in the orthorhombic phase, giving rise to the assembly of alternating high- and low-water content channels (Figures 3 and 4). The partial dehydration between 300 K and 400 K takes place mainly in the water-rich channels, and additionally, some water molecules diffuse into the water-deficient channels to form the disordered water structures (Figures 4 and 5). To the best of our knowledge, this is the first observation of an order–disorder transition in a zeolitic water assembly induced by dehydration. In aluminosilicate natrolite ( $16 H_2O$  per  $80 O_f$ ), the two water-rich phases, superhydrated natrolite ( $32 H_2O$  per  $80 O_f$ )<sup>7</sup> and ordered-

paranatrolite ( $24 H_2O$  per  $80 O_f$ ),<sup>18</sup> are formed by applying hydrostatic pressures in the presence of water in the pressure transmitting fluid and show a uniform water distribution throughout the channels. Similarly, the tetragonal potassium gallosilicate natrolite with the ambient water content of  $6H_2O$  per  $40 O_f$  becomes superhydrated ( $12 H_2O$  per  $40 O_f$ ) under hydrostatic pressure and also reveals a tetragonal symmetry, which remains stable after the pressure is released.<sup>8</sup> In a synthetic rubidium gallogermanate analogue, an anhydrous phase is formed directly by a high-pressure synthesis at 0.8 kbar and 750 °C.<sup>19</sup> We intend to investigate the possible local structural distortions during water assembly order–disorder transitions using atomic pair distribution function analysis. Further synthesis and structural studies are also needed to better understand the relationship between the zeolitic water contents and the chemistry of the natrolite framework at ambient conditions as well as in response to temperature and pressure variations.

**Acknowledgment.** This work was supported by the Korea Research Foundation Grant funded by the Korean Government (MOEHRD) (KRF-2006-D00538). S.J.K. is grateful for the support from the Korea Institute of Science and Technology (KIST). J.B.P. appreciates support from the NSF-DMR-0452444. Research carried out in part at the NSLS at BNL is supported by the U.S. DOE (DE-Ac02-98CH10886 for beamline X7A).

**Supporting Information Available:** Rietveld refinement results. This material is available free of charge via the Internet at <http://pubs.acs.org>.

JA075037Z

- (18) Lee, Y.; Hriljac, J. H.; Parise, J. B.; Vogt, T. *Am. Mineral.* **2005**, *90*, 252–257.  
 (19) Klaska, K.-H.; Jarchow, O. Z. *Kristallogr.* **1985**, *172*, 167–174.